Article

Trapezoidal Motion Profile to Suppress Residual Vibration of Flexible Object Moved by Robot

Hyun Joong Yoon [1], Seong Youb Chung [2], Han Sol Kang [2] and Myun Joong Hwang [2],*

[1] School of Mechanical and Automotive Engineering, Catholic University of Daegu, Gyeongsan 38430, Korea; yoon@cu.ac.kr
[2] Department of Mechanical Engineering, Korea National University of Transportation, Chungju 27469, Korea; sychung@ut.ac.kr (S.Y.C.); khsol0124@ut.ac.kr (H.S.K.)
* Correspondence: mjhwang@ut.ac.kr; Tel.: +82-43-841-5126

check for updates

Abstract: The residual vibration when a robot manipulator is operated at high speed needs to be suppressed. These vibrations are generated by the resonance of a flexible object being moved by the robot, and research on control algorithms and motion profiles is ongoing to reduce them. In this paper, we propose a method to reduce the residual vibration of an object moved by a robot manipulator by optimizing the acceleration/deceleration time calculated using the object's natural frequency. The relationship between acceleration/deceleration time and the residual vibration in a trapezoidal velocity profile is considered by analyzing the scenario when the jerking motion characteristic of such vibrations occurs. The results of experiments using a commercial robot show that residual vibrations can be reduced by the proposed method without the need for an additional feedback control algorithm while transferring a flexible object over small and large distances.

Keywords: industrial robot; manipulator; residual vibration; motion profile; motion control

---

1. Introduction

With trends in manufacturing innovation such as Industry 4.0, research interest in the use of robots for automation has grown in recent years [1]. Robot manipulators have been applied to a variety of tasks in industrial applications. For the precise manipulation of objects, it is important to reduce the residual vibration caused by the resonance of the robot and the object once the former reaches the target. In particular, residual vibrations can affect the quality of the robot's action and increase the time needed to complete the task, as they need to be allowed to settle once the manipulator has reached the target. To reduce the vibrations, a method of optimization that uses vibration analysis and dynamic analysis in the design can be used [2,3]. However, it is impractical to design a new robot for every task for flexible production sites. Motion control is a typical method to reduce vibrations in the robot without changing mechanical design [4]. The generation of vibrations can be influenced according to the profile of the driving motion of the robot. A well-known method of motion control creates such a smooth profile [5], and pre-filtering can be used as well [6]. However, if a commercial industrial robot is used, the user cannot add a user-made profile algorithm or pre-filtering method into the robot controller because the commercial controller for the industrial robot has closed architecture [7–9]. For safety reasons, only skilled persons can set motion parameters in the provided trajectory planning method. The method of trajectory planning used in most commercial robots uses a trapezoidal velocity profile [10,11]. For example, the operator can input the maximum velocity and acceleration of motion to set a trapezoidal velocity profile in commercial industrial robots manufactured by major robot manufacturers [7–9].

In this paper, a simple method without an additional feedback control algorithm is proposed to reduce residual vibration. It determines the acceleration/deceleration time of the trapezoidal profile to reduce residual vibration by analyzing the relationship between occurrences of the jerking motion characteristic of residual vibrations and the natural frequency at which resonance can occur during the high-speed motion of the robot. The residual vibration of a flexible object attached to a six-degree-of-freedom (DOF) manipulator is effectively shown to be reduced by determining the acceleration/deceleration time of the trapezoidal profile.

Previously proposed high-order polynomial motion profiles require large amounts of computation, and such pre-filtering methods as input-shaping technology have the disadvantage of time delay in motion completion. On the contrary, the method proposed here is based on a simple trapezoidal profile that, thus, incurs no time delay and does not require additional computation.

Section 2 introduces research related to that in this paper. The method to generate the trapezoidal motion profile is explained in Section 3, and a theoretical analysis to determine the duration of acceleration to reduce residual vibration is described in Section 4. Experiments using an industrial robot to test the proposed method are described in Section 5. Sections 6 and 7 contain the discussion and conclusion of this study, respectively.

2. Related Research

The typical methods used to reduce the vibration of a robot without changing its mechanical design are the feedback and the feedforward methods. Errors caused by vibrations are measured and compensated for by feedback control. However, there is a problem whereby the control scheme of the actuator must be modified to implement a new feedback control law. Therefore, this study focuses on feedforward methods such as motion profile generation and input shaping. The representative method is motion control, which generates a smooth motion profile. It is possible to influence the generated vibrations according to the motion profile imposed on the actuators of the robot. It is not necessary to revise or modify the control scheme for the actuators because the motion profiles are generated using the feedforward method imposed during trajectory generation.

Previous research has attempted to reduce vibrations in robots by applying various smooth velocity profiles, such as the S-curve and the jerk-bounded profile [4,5,12–16]. High-order polynomial motion profiles enable the robot to move smoothly [12,13]. As orders of a polynomial equation, the position and velocity of the robot have smooth shapes. Residual vibrations can then be reduced by smooth motion, but additional computation is needed because the order of the polynomial equation increases due to an increase in the number of coefficients as a function of time. A large acceleration and torque are also needed to move the same distance as when a trapezoidal motion profile is applied to the motion. The trapezoidal motion profile and third-order motion profile in position are compared in Figure 1 when the same magnitude of maximum velocity is applied to attain the same displacement. The duration of motion for the same displacement is shorter when trapezoidal motion is applied. In Figure 2, the change in the velocity profiles can be shown according to the order of the polynomial function. The maximum velocity and acceleration increase with the order of the function when the duration of motion is the same. Therefore, it can be inferred that the trapezoidal motion profile is effective in the magnitude of velocity and acceleration in comparison with polynomial motion profiles.

A jerk-bounded or jerk-optimized motion profile is a means of reducing residual vibration [14–16]. A jerk is the time derivative of acceleration, and quick changes to acceleration can cause jerks of large values. Therefore, some researchers have attempted to show that vibrations can be reduced by minimizing or bounding the jerk. Past research has shown the influence of an optimized trajectory or motion profile. At the same time, it is challenging to determine the jerk limit of an actuator of a robot to bound it in the planning stage.

In addition to velocity profile generation, many studies have explored shaping the motion profile generated by the input-shaping technique using a preprocessing filter [6,17,18]. The input-shaping technique proposed in reference [6] shows that vibrations can be reduced by shaping the input

according to impulse by reducing the period of vibration and damping ratio. As the implementation is simple and the results are effective for moving systems, efforts have been made to apply this to various systems. For application to robots, a learning technique was applied to industrial robots in reference [17] and vibration control of flexible robots was considered in reference [18]. However, this approach has a disadvantage whereby the time required for motion is prolonged by half the vibration period. To compensate for this, negative input shaping has been proposed in reference [19], but has been applied to only simple systems, such as a crane, and has not yet been tested on a complex system, such as a multi-DOF robot.
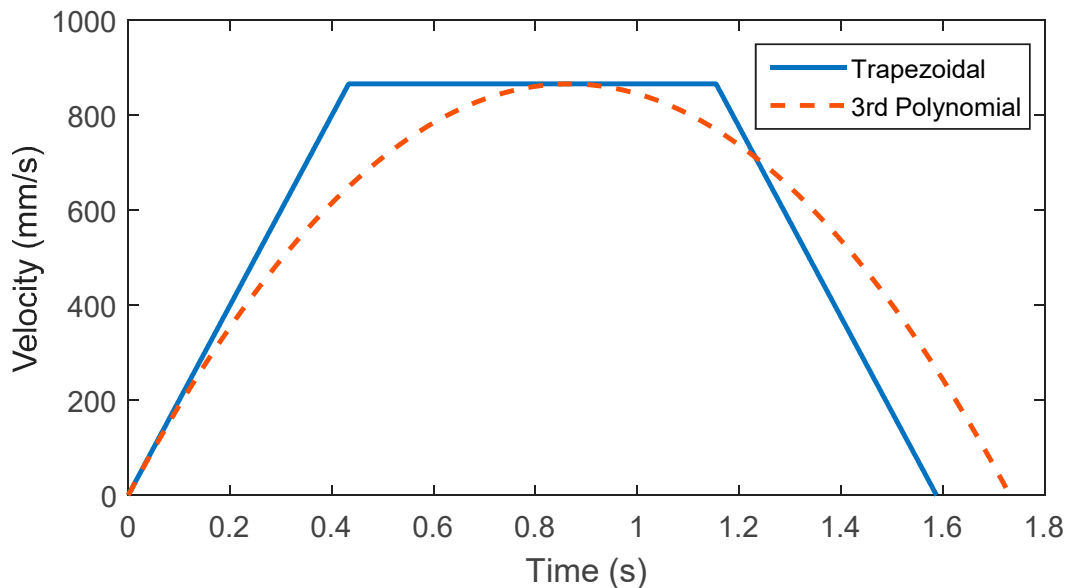

Figure 1. Comparison of trapezoidal motion profile and 3rd-order polynomial trajectory with the same maximum velocity and acceleration.
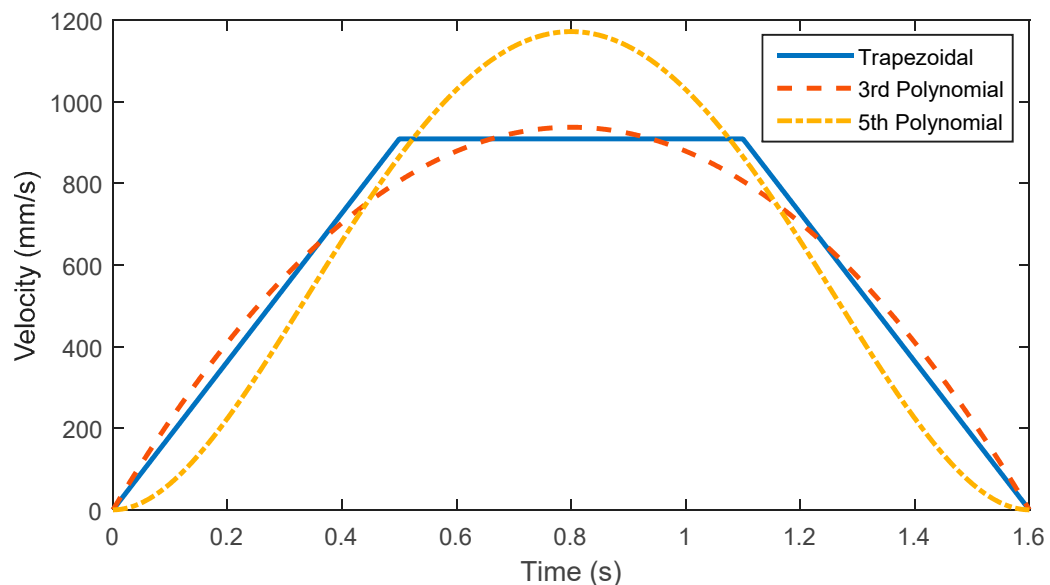

Figure 2. Comparison of trapezoidal motion profile, 3rd-order polynomial trajectory, and 5th-order polynomial trajectory with the same duration of motion.

To simplify the design of the motion profile and easily apply it to various robot systems, it is necessary to examine ways of reducing vibrations based on a trapezoidal velocity profile, which is the simplest motion profile. For this purpose, research has been conducted on the design of the trapezoidal

profile. Ha et al. [20] showed vibrations can be reduced using a trapezoidal profile by simulating a case where the travel distance was sufficiently large for one-DOF motion. In the trapezoidal profile, the points of acceleration and deceleration indicate zero in control system analysis, and residual vibrations can be reduced by the pole-zero offset effect depending on the point of the pole, which represents the mode of vibration of the system. However, the authors did not verify their proposal on a robot system and did not consider small distances.

In this paper, we propose a method to design a trapezoidal profile that can reduce the vibrations of a six-DOF industrial robot as it transports a flexible object. Experimental verification was performed for various cases, including one where the displacement was long and one where it was short. Experiments were carried out both when the robot configuration was changed during operation and when it was not.

3. Design of Trapezoidal Velocity Profile

The trapezoidal motion profile is considered here for moving robots. It has a trapezoidal shape at the velocity level, and is known as the linear-segment-with-parabolic-blend (LSPB) trajectory [7,8]. The trapezoidal motion profile is divided into three sections: acceleration, constant velocity, and deceleration, respectively. If the displacement is positive, the acceleration is positive and constant in the first section. The velocity is then a linear function of time and position is a parabolic curve of time. In the Section 2, acceleration is zero and the velocity has a constant value. Therefore, the position is a linear function of time in this section. Finally, a constant negative acceleration is imposed in the third section and velocity is linearly reduced. Figure 3 shows the position, velocity, and acceleration of the trapezoidal motion profile, where the three sections are shown.
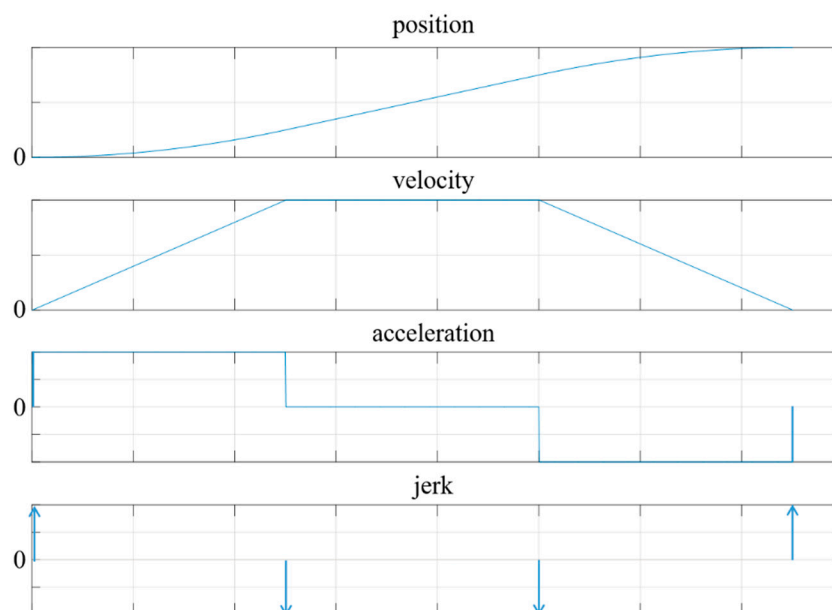

Figure 3. Trapezoidal motion profile.

To plan a trapezoidal motion profile, the parameters of motion should be pre-assigned and the displacement given. If the maximum velocity and acceleration are given, the duration of acceleration and motion can be derived. Usually, the operator can assign the maximum values of velocity and acceleration to set the motion parameters in a commercial industrial robot [9–11]. It is assumed that velocities at the starting and end points are zero as shown in Figure 4, and that the acceleration and deceleration times are identical. If the maximum velocity is v_{max} and the maximum acceleration is a_{max}, acceleration time t_a can be derived as (1). The displacement is defined as Δx and assumed to be positive. The time required to reach the target by moving by Δx is t_f, and can be computed by

(2). If the acceleration and deceleration are symmetric, the duration for which constant velocity is maintained is derived as in (3).

$$t_a = \frac{v_{max}}{a_{max}} \tag{1}$$

$$t_f = \frac{\Delta x}{v_{max}} + t_a \tag{2}$$
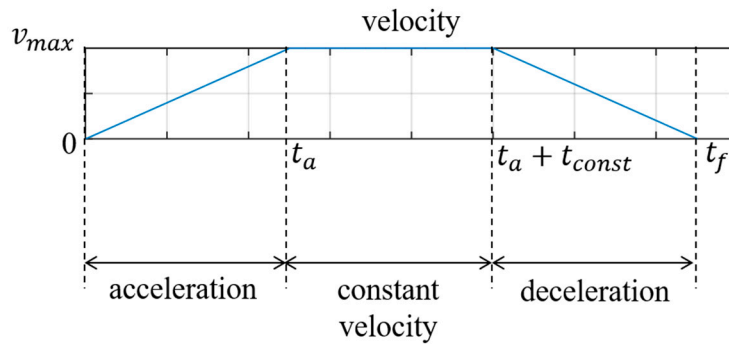
$$t_{const} = t_f - 2t_a \tag{3}$$

Figure 4. Three sections of trapezoidal motion profile.

In (3), t_{const} is positive when t_f is greater than $2t_a$. This means that t_{const} can be zero or negative if t_f is identical to or smaller than $2t_a$. This happens when the displacement, Δx, is relatively short. The constant velocity zone may not exist, and only acceleration and deceleration zones appear as shown in Figure 5. The maximum velocity is not reached if the maximum acceleration, a_{max}, is imposed in this case. Therefore, t'_a, t'_f, and v'_{max} need to be recalculated. The relation between t'_a and v'_{max} is as shown in (4). Δx can then be represented as (5). In (6), t'_a can be calculated using Δx and a_{max} which are given for trajectory planning. The maximum velocity, v'_{max}, can be derived by (7) by substituting (6) into (4), but this is smaller than the pre-assigned maximum velocity. t'_f is the twice of t'_a as in (8).

$$t'_a = \frac{v'_{max}}{a_{max}} \tag{4}$$

$$\Delta x = t'_a \cdot v'_{max} = t'^2_a \cdot a_{max} \tag{5}$$

$$t'_a = \sqrt{\frac{\Delta x}{a_{max}}} \tag{6}$$

$$v'_{max} = a_{max} \cdot t'_a = \sqrt{a_{max} \cdot \Delta x} \tag{7}$$

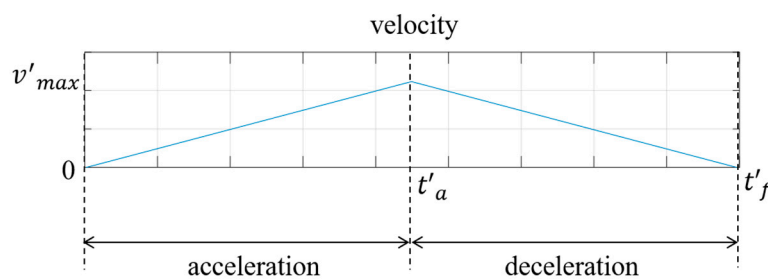$$t'_f = 2t'_a = \sqrt{\frac{4\Delta x}{a_{max}}} \tag{8}$$

Figure 5. Short-pitch trapezoidal motion profile.

4. Profiles for Reducing Residual Vibration

Residual vibration may occur due to resonance during high-speed motion control of the robot, and the generation of jerks can change the shape of the residual vibrations. The jerk, which is the first derivative of acceleration, is a factor in the system because it influences the mechanism. Therefore, jerking occurs when the robot is driven by its mechanism. We analyze the relationship between the time of occurrence of the jerk and the natural frequency at which the resonance can occur. In the case of a trapezoidal velocity profile, the jerk occurs at the beginning and end of acceleration/deceleration as shown in Figure 3.

In the acceleration section, a positive jerk from a positive impulse generated at the start of acceleration generates vibration, and a negative jerk, which is generated when the acceleration is terminated and the system transitions to the constant velocity section, generates a vibration with the opposite phase. Therefore, when the interval between these points is half the vibration period, which is the reciprocal of the natural frequency as shown in Figure 6, the amplitude of the two vibrations is added and the residual vibration is amplified. On the contrary, if the acceleration interval is equal to the oscillation period, as shown in Figure 7, the amplitudes of the two oscillations have different signs, resulting in a cancelation of the residual oscillation.
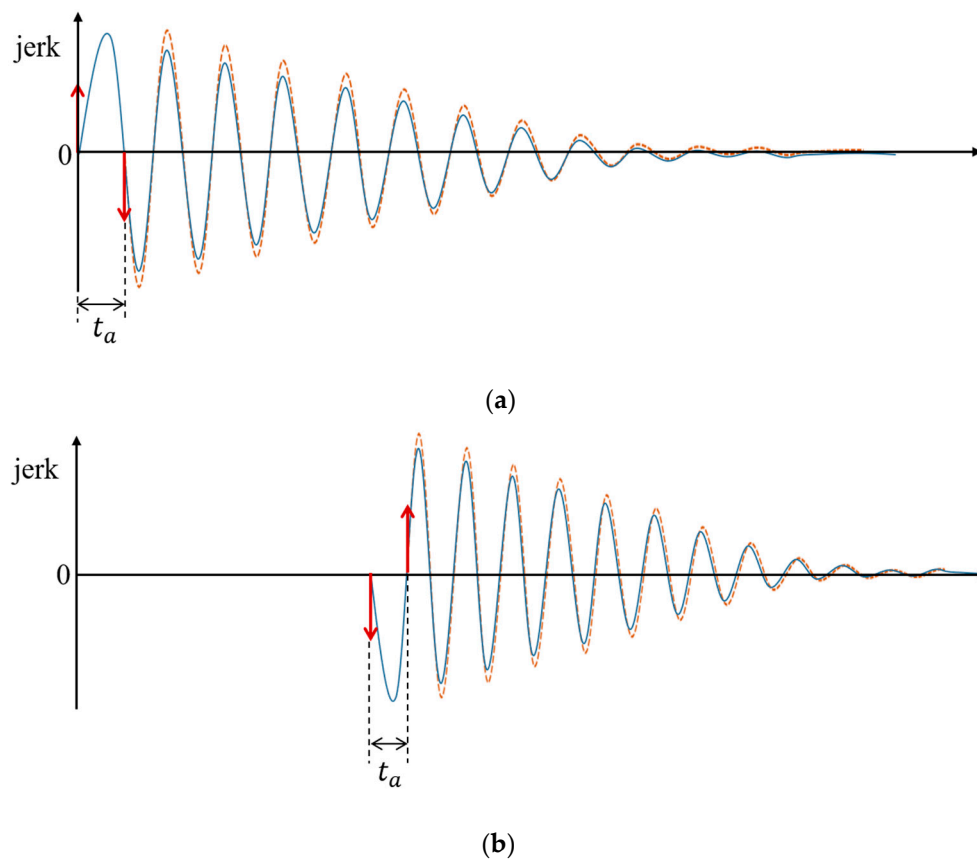

(**a**)

(**b**)

Figure 6. The case where residual vibrations caused by two jerks are amplified: (**a**) in acceleration phase; (**b**) in deceleration phase.
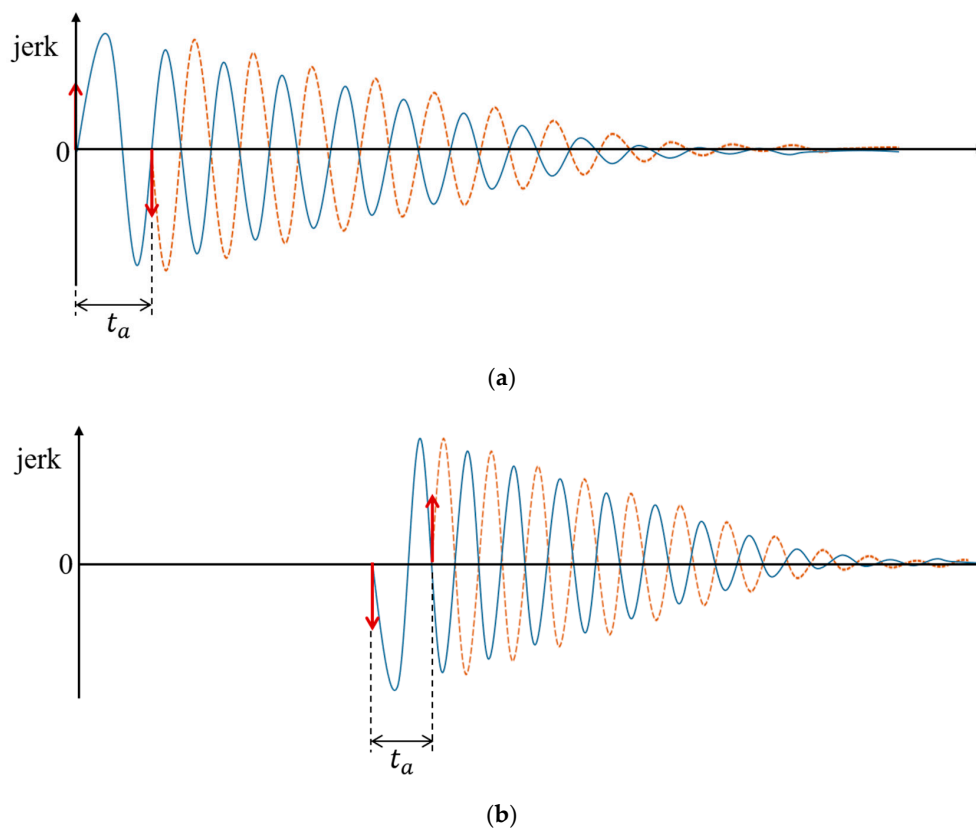
(a)

(b)

Figure 7. The case where the residual vibrations caused by two jerks are eliminated: (**a**) in acceleration phase; (**b**) in deceleration phase.

The residual vibration is canceled when the interval t_a of the acceleration period is equal to or a multiple of the period $T_{vibration}$ corresponding to the natural frequency of the object as shown in (9) and (10). Moreover, as the same principle is applied to the deceleration section, the residual vibration can be reduced when acceleration time, t_a, and deceleration time, t_d, are multiples of the period corresponding to the natural frequency:

$$T_{vibration} = \frac{1}{f_{natural}} \tag{9}$$

$$t_a = t_d = k \cdot T_{vibration}, \ where \ k = 1, 2, \cdots \tag{10}$$

5. Experiments

The proposed methods were investigated on a commercial industrial robot. A flexible beam was attached to the end-effector of the robot, and the amplitude and settling time of the residual vibrations were measured when it was moved quickly. The settling time in this paper is defined as the duration from the arrival time in the target position to the time when the amplitude of residual vibration is within ± 1.5 mm.

5.1. Experimental Setup and Target Task

A steel cantilever 300 mm long and 1 mm thick was used as an object moved by the robot. To measure the natural frequency of the target system, the acceleration sensor MPU-6050 was attached to the end of the cantilever coupled with the robot, and acceleration was measured using the cantilever. The measured values were analyzed using the fast Fourier transform (FFT). The natural frequency of the cantilever calculated using measurements was approximately 8 Hz. Experiments were conducted on a six-DOF commercial articulated robot with a cantilevered beam that could generate residual

vibrations. The robot was an IRB120 model manufactured by ABB [7]. A high-speed camera at 240 fps was installed to photograph the residual vibrations at the point of arrival of the robot as shown in Figure 8.
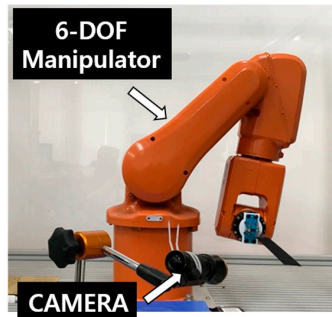

Figure 8. Experimental setup.

Two types of task were performed using the robot system and three kinds of motion profiles were tested for each. The first task consisted of rotating only axis-1 without changing configuration. In the first task, the natural frequency of the robot was constant because its inertia was constant. The second task featured a change in the inertia of the robot during motion. Its end-effector linearly moved along the diagonal direction in the task space, because of which its configuration kept changing. The moving distance is selected so that the constant velocity section can be included within the workspace or joint limit of the robot. The maximum velocity is chosen by referring to the manual of the robot.

5.2. Constant Configuration

The cases where the acceleration/deceleration time was a multiple of the vibration period corresponding to the natural frequency of 8 Hz, and those where time was not a multiple were compared while the robot linearly moved 500 mm at a maximum velocity of 1000 mm/s. The start position (x, y, z) was (277.9, −250.3, 630) in mm as shown in Figure 9a and the goal was (374, 0, 630) as shown in Figure 9b. The velocity profiles of the robot are shown in Figure 10. All four cases were tested in the experiment, and were classified according to the acceleration times listed in Table 1. The results in terms of amplitude and settling time for all cases are shown in Table 1. Figure 11 shows measured photos of the maximum deviation at the target. The amplitude and settling time in cases 2 and 4, where the acceleration/deceleration time was a multiple of the vibration period of the natural frequency, were smaller than those in cases 1 and 3. The best in terms of the suppression of residual vibration was case 4. where the duration of acceleration was twice the vibration period. Comparing the best result with the worst result, the amplitude is reduced by 94.6% and the settling time is reduced by 7.75 s. In case 4, the settling time is zero because the magnitude of overshoot is below ±1.5 mm after reaching the goal position.

(**a**)

(**b**)

Figure 9. The experiment in which the robot moved with a constant configuration: (**a**) initial position; (**b**) final position.
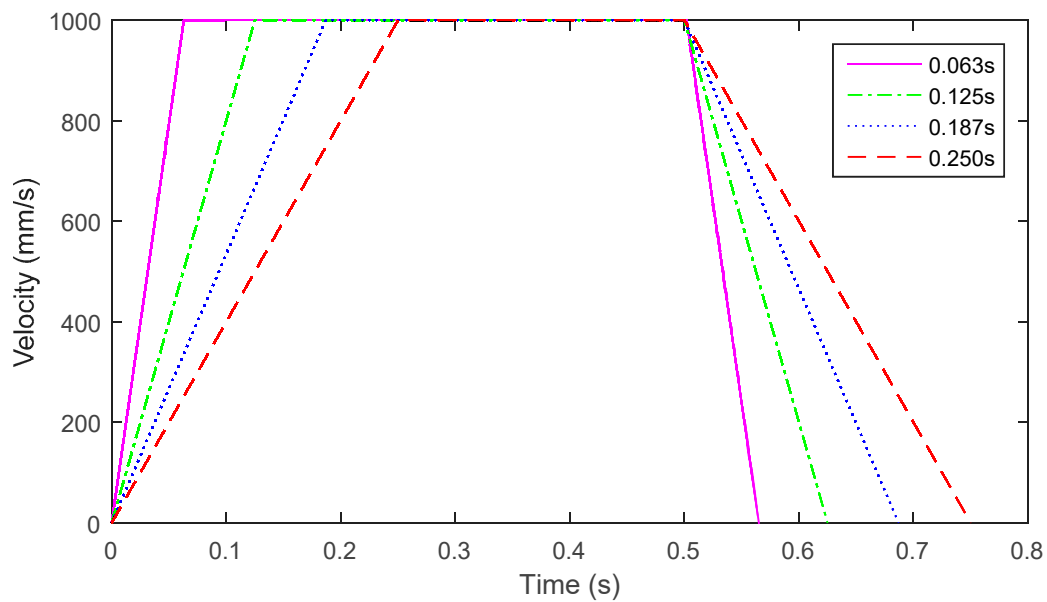
Figure 10. The velocity profiles when the robot moved 500 mm with a maximum velocity of 1000 mm/s.

Table 1. Experimental results of maximum amplitude and settling time when the robot moved 500 mm with a maximum velocity of 1000 mm/s.

	t_a, t_d (s)	t_{const} (s)	Max. Amplitude (mm)	Settling Time (s)
Case 1	0.063	0.439	37	7.75
Case 2	0.125	0.375	5	0.875
Case 3	0.187	0.313	16	4.375
Case 4	0.250	0.250	2	0

(**a**)

(**b**)

Figure 11. Position deviations at target point: (**a**) when $t_a = 0.063$; (**b**) when $t_a = 0.250$.

In the first experiment, the maximum velocities were identical for all cases, but the time taken to move was longer in case 4. To test the influence of the maximum velocity, motion profiles using the same time to move were designed as shown in Figure 12. The velocity in case 4 was then the largest. The amplitude and settling time in cases 2 and 4, in which the acceleration/deceleration time was a multiple of the vibration period of the natural frequency, were smaller than those in cases 1 and 3. The best cases in terms of the suppression of residual vibration were cases 2 and 4 when the duration of acceleration was identical to or twice the vibration period as shown in Table 2. Comparing the best result with the worst result, the amplitude is reduced by 95.0% and the settling time is reduced by 8.375 s. The maximum deviations at the target were compared as shown in Figure 13.
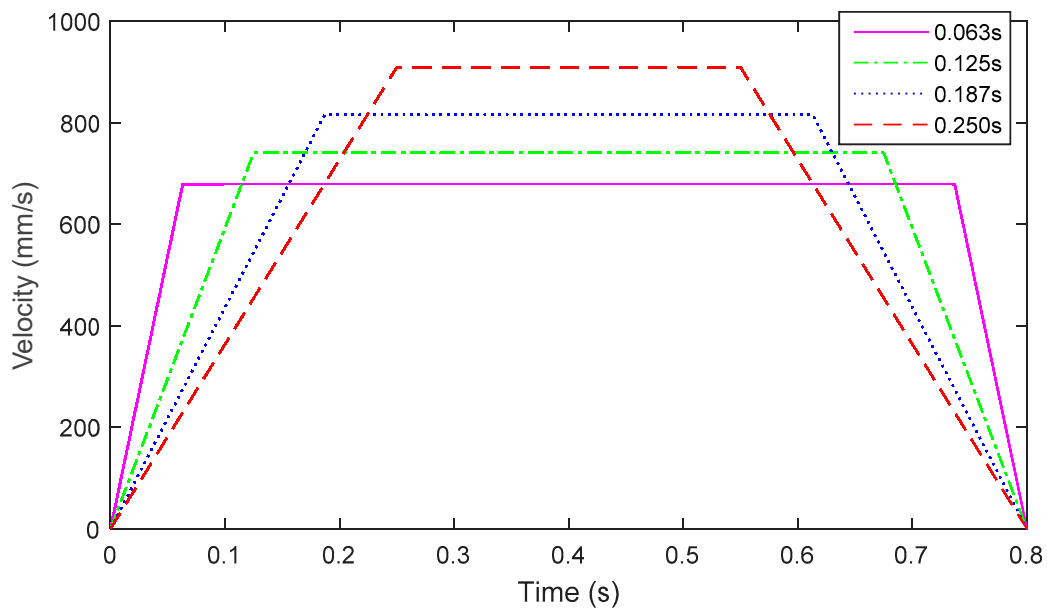
Electronics **2019**, 8, 30

10 of 17

Figure 12. The velocity profiles when moving 500 mm over 0.8 s.

Table 2. Experimental results of maximum amplitude and settling time when moving 500 mm over 0.8 s.

	t_a, t_d (s)	t_{const} (s)	Max. Amplitude (mm)	Settling Time (s)
Case 1	0.063	0.674	40	8.375
Case 2	0.125	0.550	2	0
Case 3	0.187	0.462	22	5.375
Case 4	0.250	0.300	2	0

(**a**)　　　　　　　　　　　　　(**b**)

Figure 13. Position deviations at target: (**a**) when $t_a = 0.063$; (**b**) when $t_a = 0.250$.

If the moving distance was short while the duration of acceleration was kept constant, the trapezoidal velocity profile could not be formed. Instead, the triangular velocity profile was designed as shown in Figure 14. The detailed results are listed in Table 3. In this experiment, case 2 was the best, where the duration of acceleration was identical to the period of vibration. Figure 15 shows photos of the maximum deviation at the target. The results show that the residual vibration was effectively reduced when the duration of acceleration was identical to or a multiple of the period of vibration. Comparing the best result with the worst result, the amplitude is reduced by 94.5% and the settling time is reduced by 11.5 s.
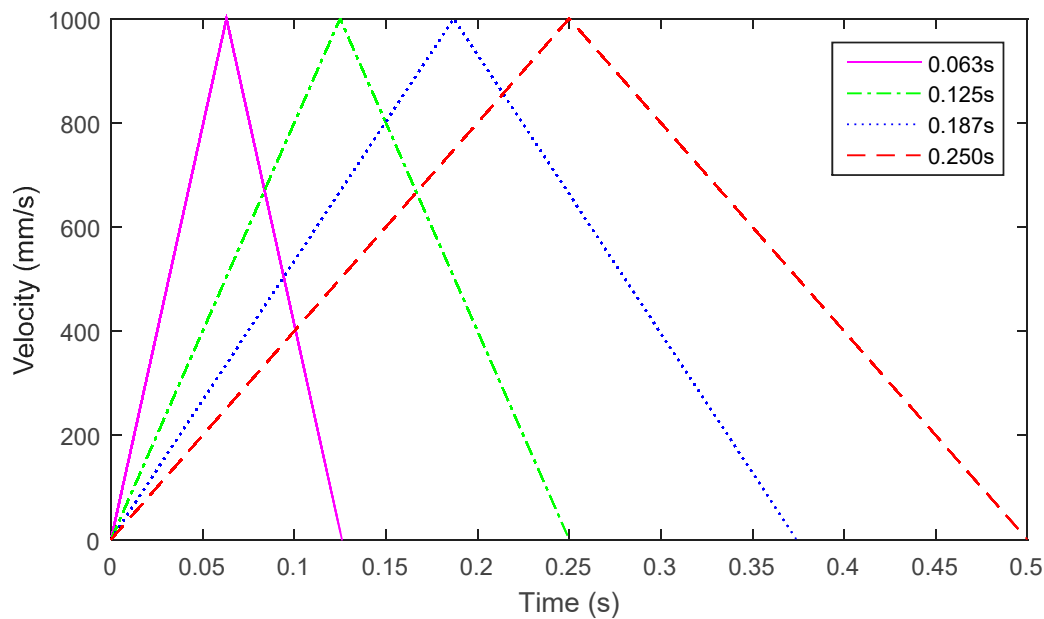
Figure 14. The velocity profiles when moving a short distance with a maximum velocity of 1000 mm/s.

Table 3. Experimental results for maximum amplitude and settling time when moving a short distance with a maximum velocity of 1000 mm/s.

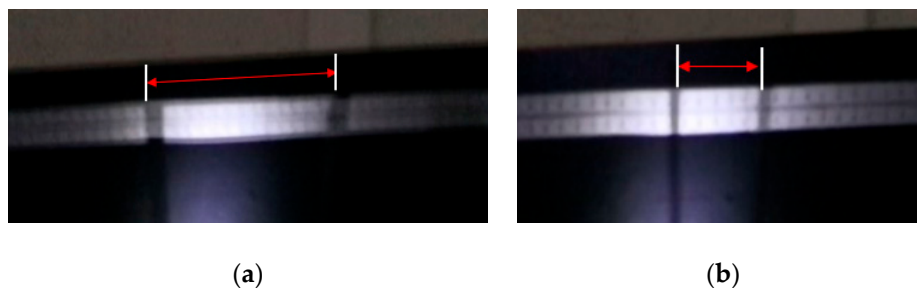|	t_a, t_d (s)	Distance (mm)	Max. Amplitude (mm)	Settling Time (s)
Case 1	0.063	62.5	55	11.5
Case 2	0.125	125	3	0
Case 3	0.187	187.5	17	7.25
Case 4	0.250	250	5	1.875

Figure 15. Position deviations at target: (**a**) when $t_a = 0.063$; (**b**) when $t_a = 0.250$.

5.3. Changing Configuration

The second task consisted of the robot moving linearly over 425 mm with a maximum velocity of 1000 mm/s. The robot moved diagonally in the task space. The start position (x, y, z) was (0, −196.3, 586.2) in mm as shown in Figure 16a and the goal position was (377, 0, 586.2) as shown in Figure 16b. In this case, the configuration of the robot changed during motion, as did its natural frequency.

The velocity profiles of the robot are shown in Figure 17. All four cases were tested in the experiment. The results in terms of amplitude and settling time for all cases are listed in Table 4. Figure 18 shows photos of the maximum deviation at the target. The amplitude and settling time in cases 2 and 4, in which the acceleration/deceleration time was a multiple of the vibration period of the natural frequency, were smaller than those in cases 1 and 3. The best case in terms of the suppression of residual vibration was case 2, wherein the duration of acceleration was identical to the vibration period. Comparing the best result with the worst result, the amplitude is reduced by 73.1% and the settling time is reduced by 6.125 s.
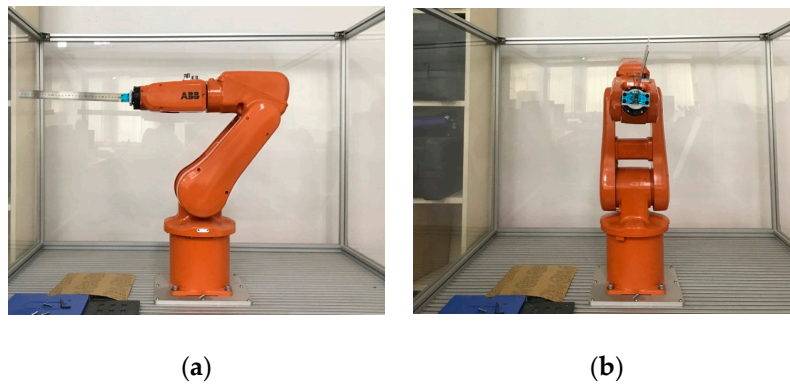
(a) **(b)**

Figure 16. The experiment where the robot linearly moved while the configuration changed: (**a**) initial position; (**b**) final position.
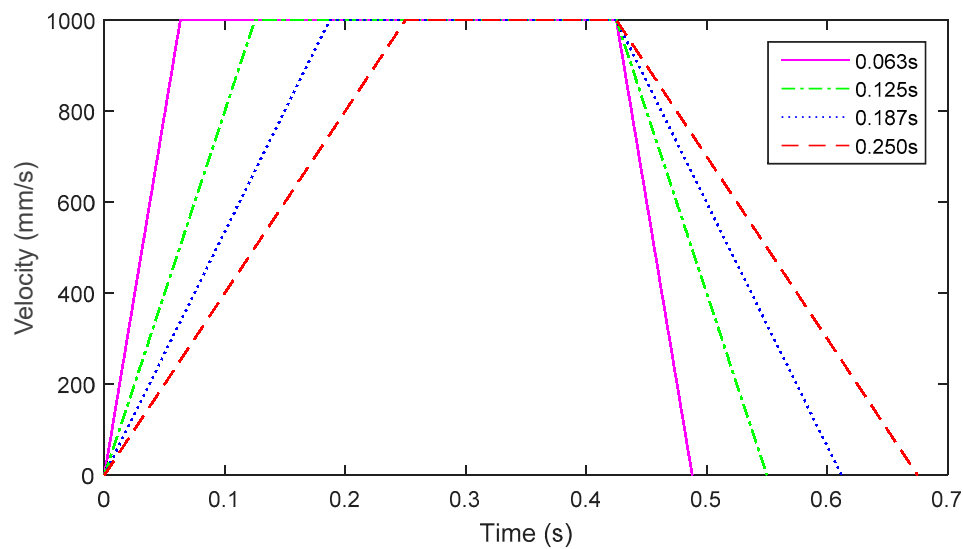

Figure 17. The velocity profiles when moving 425 mm with a maximum velocity of 1000 mm/s.

Table 4. Experimental results of maximum amplitude and settling time when moving 425 mm with a maximum velocity of 1000 mm/s.

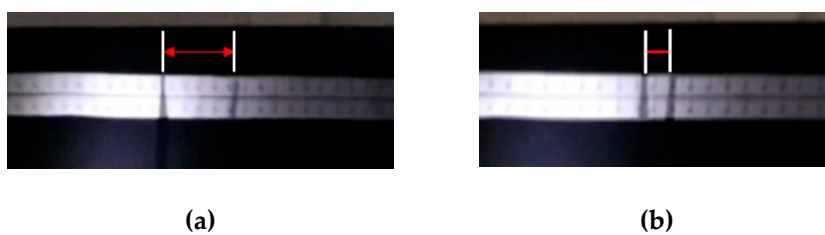|	t_a, t_d (s)	t_{const} (s)	Max. Amplitude (mm)	Settling Time (s)
Case 1	0.063	0.362	26	7.625
Case 2	0.125	0.300	7	1.5
Case 3	0.187	0.238	10	5.25
Case 4	0.250	0.175	7	4.875

(a) **(b)**

Figure 18. Position deviations at target: (**a**) when $t_a = 0.063$; (**b**) when $t_a = 0.250$.

To determine the influence of maximum velocity for residual vibration, motion profiles with the same time taken to move were designed as shown in Figure 19. The velocity in case 4 was then the largest. The amplitude and settling time in cases 2 and 4, in which the acceleration/deceleration time

was a multiple of the vibration period of the natural frequency, were smaller than those in cases 1 and 3. Case 2 was the best in terms of suppression of residual vibration when the duration of acceleration was identical to the vibration period. Comparing the best result with the worst result, the amplitude is reduced by 90.3% and the settling time is reduced by 7.25 s. The maximum deviations at the target are compared in Figure 20.
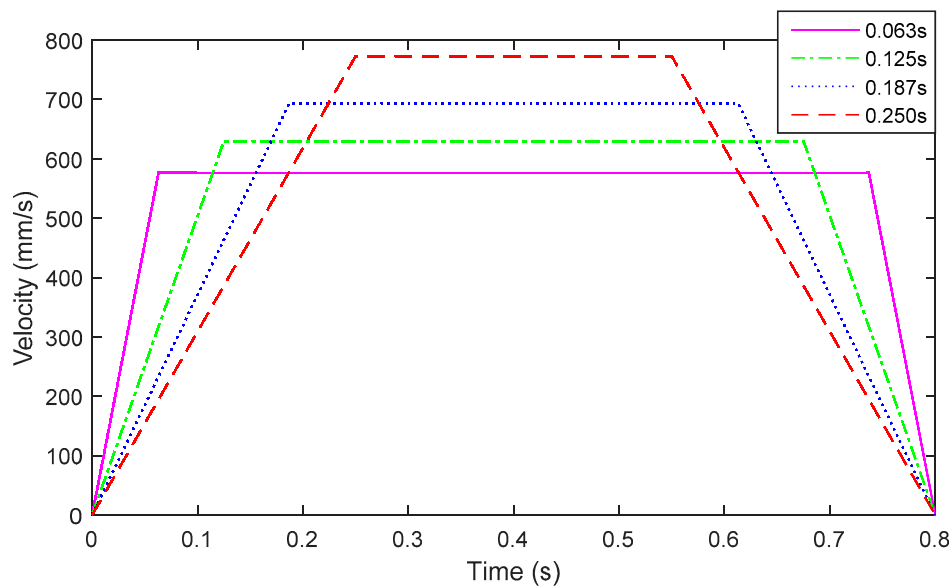

Figure 19. The velocity profiles when moving 425 mm over 0.8 s.

(**a**)   (**b**)

Figure 20. Position deviations at target: (**a**) when $t_a = 0.063$; (**b**) when $t_a = 0.250$.

In Table 4, it can be shown that the settling time is relatively long in case 4 compared with the case 4 in Table 5. The reason is that the time of the constant velocity section, t_{const}, is smaller than the acceleration/deceleration time in case 4 of Table 4. In this case, the residual vibration generated in the acceleration section is not sufficiently reduced within the constant velocity section, so it can be added to the residual vibration due to the deceleration section. The duration of the constant velocity zone should not be less than time period corresponding to the natural frequency.

Table 5. Experimental results of maximum amplitude and settling time when moving 425 mm over 0.8 s.

	t_a, t_d (s)	t_{const} (s)	Max. Amplitude (mm)	Settling Time (s)
Case 1	0.063	0.674	31	7.25
Case 2	0.125	0.550	3	0
Case 3	0.187	0.426	19	5.625
Case 4	0.250	0.300	6	2.625

The triangular velocity profiles in Figure 21 were imposed on the robot to check its movement over a short distance. The results are listed in Table 6. In this experiment, case 2 was the best, where the

duration of acceleration was identical to the vibration period. Figure 22 shows photos of the maximum deviation at the target. The results show that the residual vibration was effectively reduced when the duration of acceleration was identical to or a multiple of the vibration period. Comparing the best result with the worst result, the amplitude is reduced by 94.7% and the settling time is reduced by 13.0 s.
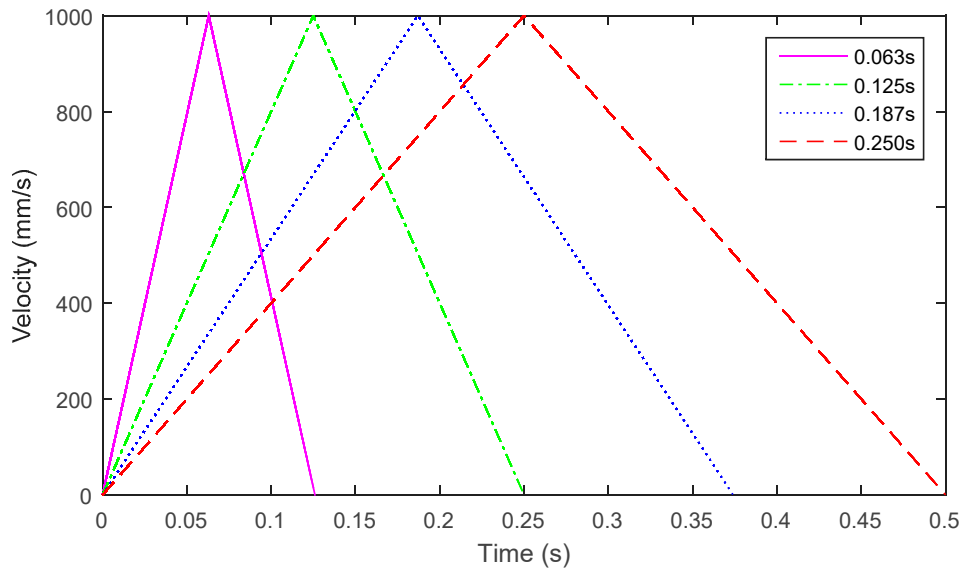

Figure 21. The velocity profiles when moving a short distance with a maximum velocity of 1000 mm/s.

Table 6. Experimental results of maximum amplitude and settling time when moving a short distance with a maximum velocity of 1000 mm/s.

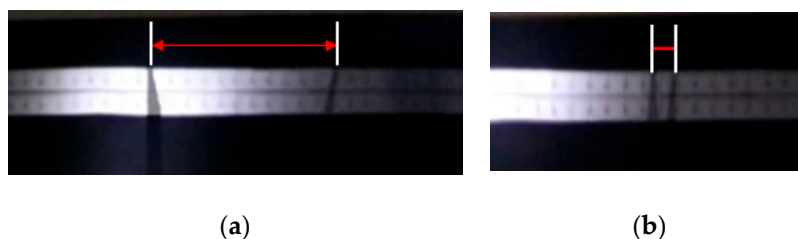|	t_a, t_d (s)	Distance (mm)	Max. Amplitude (mm)	Settling Time (s)
Case 1	0.063	62.5	57	13
Case 2	0.125	125	3	0
Case 3	0.187	187.5	19	10.625
Case 4	0.250	250	5	5.5

(**a**)　　　　　　　　　　　　　　　　　　　　　　(**b**)

Figure 22. Position deviations at target: (**a**) when $t_a = 0.063$; (**b**) when $t_a = 0.250$.

The experimental results using a flexible beam attached to the six-DOF industrial robot manipulator show that residual vibration caused by the motion profile imposed on the robot manipulator can be reduced by setting the acceleration/deceleration time to be identical to or twice the period corresponding to the natural frequency of the given object. Furthermore, the proposed method can be applied to cases where the configuration of the robot does and does not change while moving flexible objects.

6. Discussion

We conducted simulation to compare the proposed method with IST (Input Shaping Technique) in reference [6] and the natural frequency of the target system is assumed to be 8 Hz. It is assumed that the system is moved by 100 mm in 3 s. In Figure 23a, the results for three cases are represented.

The first and second cases are when the acceleration time is equal to half of the period corresponding to the natural frequency and equal to the period, respectively. The third one is the result when the IST is applied to the motion. The system reaches the target point at 3 s in the first and second case but time delay exists to arrive at the target point when IST is applied in the third case. If the results at 3 s is expanded in Figure 23b, there is about 0.06 s of delay time to reach the target point. It is a half of the time period 0.125 s, that is reciprocal of 8 Hz of the natural frequency. Also, we can determine that the residual vibration is reduced more quickly when the acceleration time is equal to the vibration period.
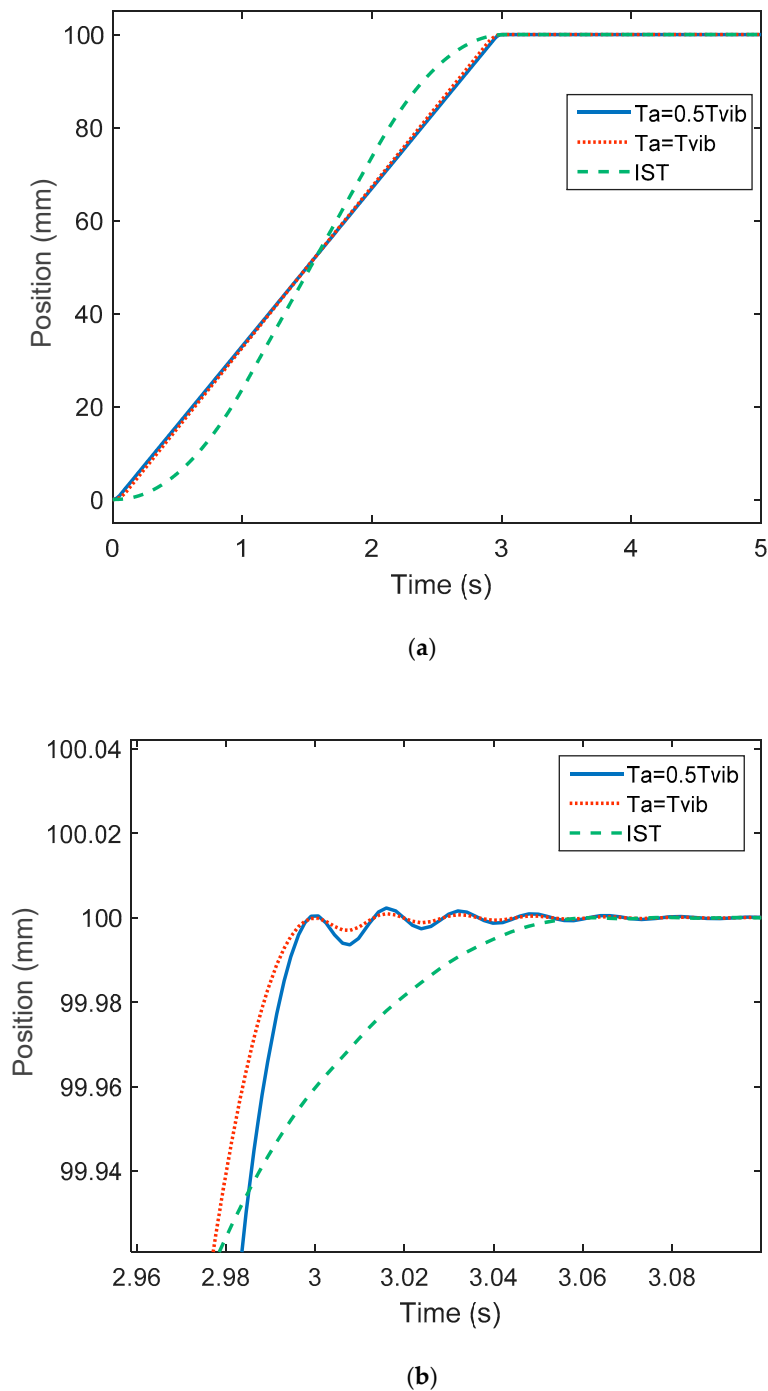

(**a**)

(**b**)

Figure 23. Comparison of residual vibration when the proposed method is applied and the IST is applied: (**a**) trajectory; (**b**) residual vibrations.

7. Conclusions

In this paper, we proposed a method to reduce the residual vibration in a robot by setting its acceleration/deceleration time. A jerk is the first derivative of its acceleration, and can be applied as an impulse-type input to the target system. By exploring this idea, the time between the occurrences of jerks in the trapezoidal motion profile was analyzed to reduce the vibrations generated by them. The duration between jerks corresponded to the time for the acceleration and the deceleration sections. It was confirmed that the residual vibration can be reduced when the interval is equal to or a multiple of the period of vibration corresponding to the natural frequency of the given object. Experiments were carried out featuring the motion of a six-DOF industrial robot manipulator equipped with a flexible beam at a frequency of 8 Hz. The experiments were performed for cases involving the same velocity and those of the same time taken to move where the acceleration/deceleration time was a multiple of the vibration period. The results show that that the amplitude and settling time of residual vibration was reduced by 73.1~95.0% in the maximum amplitude and by 6.125 s~13.0 s in settling time where the acceleration/deceleration time was a multiple of the vibration period. In designing trapezoidal profile, it is shown that the duration of the constant velocity zone should be longer than the time period corresponding to the natural frequency. This is because the residual vibration generated in the acceleration section can be added to the residual vibration due to the deceleration section if the duration of the constant velocity zone is short. If the moving distance was short, a triangular motion profile was generated with no constant velocity section. It was confirmed that vibration can be reduced, as in the case of applying a general trapezoidal profile even when a constant velocity section does not exist.

In this method, the trapezoidal profile used mainly for industrial robots was used as is, and a method to determine the acceleration/deceleration time, to design the robot, was directly applied to reduce vibrations. Unlike the input-shaping method, which is mainly applied to simple systems such as a crane, this method has the advantage of no time delay. It is shown that the acceleration/deceleration time is designed based on one dominant frequency and it is effective in reducing the residual vibration by implementing the experiment using the industrial robot. This is a limitation caused by targeting trapezoidal velocity motion profiles that are commonly applied to industrial robots.

In future work, more experiments will be conducted to test the application of the proposed method to a variety of multi-DOF robots. We will also study a method that can be extended to the case where the natural frequency of the object is unknown and will extend the proposed method to the case of considering multiple resonant frequencies.

Author Contributions: Conceptualization, H.J.Y, S.Y.C., and M.J.H.; Methodology, H.J.Y, S.Y.C., and M.J.H.; Experiment, H.S.K.; Analysis, S.Y.C. and H.S.K.; Writing-Original Draft Preparation and Revision, H.J.Y and M.J.H.; Supervision, S.Y.C. and M.J.H.; Funding Acquisition, M.J.H.

References

1. Lu, Y. Industry 4.0: A survey on technologies, applications, and open research issues. *J. Ind. Inf. Integr.* **2017**, *6*, 1–10. [CrossRef]
2. Kim, J.W.; Park, F.C.; Kim, M.S. Geometric design tools for stiffness and vibration analysis of robotic mechanism. In Proceedings of the IEEE International Conference on Robotics and Automation (ICRA), San Francisco, CA, USA, 24–28 April 2011; pp. 1942–1947.
3. Dwivedy, S.K.; Eberhard, P. Dynamic analysis of flexible manipulators, a literature review. *Mech. Mach. Theory* **2006**, *41*, 749–777. [CrossRef]
4. Li, H.; Le, M.D.; Gong, Z.M.; Lin, W. Motion profile design to reduce residual vibration of high-speed positioning stages. *IEEE/ASME Trans. Mechatron.* **2009**, *14*, 264–269. [CrossRef]

5.   Nguyen, K.D.; Ng, T.; Chen, I. On algorithms for planning S-curve motion profiles. *Int. J. Adv. Robot. Syst.* **2008**, *5*, 99–106. [CrossRef]

6.   Singer, N.C.; Seering, W.P. Preshaping command inputs to reduce system vibration. *ASME J. Dyn. Syst. Meas. Control* **1990**, *112*, 76–82. [CrossRef]

7.   ABB Robot Technical Reference Manual. Available online: https://library.abb.com/en/ (accessed on 9 November 2018).

8.   Mitsubishi Robot Controller Instruction Manual. Available online: http://www.mitsubishirobots.com/manuals.html (accessed on 9 November 2018).

9.   Denso Robot User Manuals. Available online: https://densorobotics.com/content/user_manuals/19/000535.html (accessed on 9 November 2018).

10.   Biagiotti, L.; Mechiorri, C. *Trajectory Planning for Automatic Machines and Robots*, 2nd ed.; Springer: Berlin, Germany, 2008; pp. 62–76, ISBN 978-3-540-85628-3.

11.   Sciavicco, L.; Siciliano, B. *Modelling and Control of Robot Manipulators*, 2nd ed.; Springer: London, UK, 2003; pp. 186–192, ISBN 1-85233-221-2.

12.   Boryga, M.; Grabos, A. Planning of manipulator motion trajectory with higher-degree polynomials use. *Mech. Mach. Theory* **2009**, *44*, 1400–1419. [CrossRef]

13.   Guan, Y.; Yokoi, K.; Stasse, O.; Kheddar, A. On robotic trajectory planning using polynomial interpolations. In Proceedings of the IEEE International Conference on Robotics and Biomimetics (ROBIO), Shatin, China, 5–9 July 2005; pp. 111–116.

14.   Huang, J.; Hu, P.; Wu, K.; Zeng, M. Optimal time-jerk trajectory planning for industrial robots. *Mech. Mach. Theory* **2018**, *121*, 530–544. [CrossRef]

15.   Perumaal, S.; Jawahar, N. Synchronized trigonometric s-curve trajectory for jerk-bounded time-optimal pick and place operation. *Int. J. Robot. Autom.* **2012**, *27*, 385–395. [CrossRef]

16.   Gasparetto, A.; Zanotto, V. A technique for time-jerk optimal planning of robot trajectories. *Robot. Comput.-Integr. Manuf.* **2008**, *24*, 415–426. [CrossRef]

17.   Park, J.; Chang, P.H.; Park, H.S.; Lee, E. Design of learning input shaping technique for residual vibration suppression in an industrial robot. *IEEE/ASME Trans. Mechatron.* **2006**, *11*, 55–65. [CrossRef]

18.   Mohamed, Z.; Tokhi, M.O. Command shaping techniques for vibration control of a flexible robot manipulator. *Mechatronics* **2004**, *14*, 69–90. [CrossRef]

19.   Singhose, W.E.; Seering, W.P.; Singer, N.C. Time-optimal negative input shapers. *ASME J. Dyn. Syst. Meas. Control* **1997**, *119*, 198–205. [CrossRef]

20.   Ha, C.W.; Rew, K.H.; Kim, K.S. Robust zero placement for motion control of lightly damped systems. *IEEE Trans. Ind. Electron.* **2013**, *60*, 3857–3864. [CrossRef]